Los Alamos National Laboratory is operated by the University of California for the United States Department of Energy under contract W-7405-ENG-36

TITLE Numerical Simulations of Long-Range Pollutant Transport From Coast to Inland Mountainous Region

LA-UR--88-113

DE88 005383

AUTHOR(S) Tetsuji Yamada, Susan S. Bunker, Elizabeth Niccum

SUBMITTED TO 8th Symposium on Turbulence and Diffusion of the American Meteorological Society

Los Alamos National Laboratory
Los Alamos, New Mexico 87545

FORM NO. 836 R4
ST. NO. 2629 5/81

NUMERICAL SIMULATIONS OF LONG-RANGE POLLUTANT TRANSPORT FROM COASTAL TO INLAND MOUNTAINOUS REGIONS

T. Yamada, S. Bunker and E. Niccum

1. INTRODUCTION

Kurita and Ueda (1986) presented an example of the long-range transport of pollutants which frequently occurs in summer in Japan under light gradient wind conditions. High concentrations of photochemical oxidants were observed in late evenings in the mountainous region approximately 160 km northwest from the large industrial zone located along the Tokyo Bay. Pollutants were apparently transported by the large-scale circulations produced by the combination of southwesterly valley winds induced by thermal lows located in the mountain ranges, and southerly sea-breeze circulations in the Pacific Ocean coastal region (Kurita et al., 1985).

We wish to simulate and evaluate the relative importance of these circulations by using a time dependent, three-dimensional mesoscale model, HOTMAC, High Order Turbulence Model for Atmospheric Circulations. The model equations of HOTMAC and numerical procedures are given in the following section. The modeled winds are compared with the observations in section 3.

2. HOTMAC

The basic equations for HOTMAC for mean wind, temperature, mixing ratio of water vapor, and turbulence are similar to those used by Yamada (1981, 1985). Surface boundary conditions are constructed from the empirical formulas by Dyer and Hicks (1970) for nondimensional wind and temperature profiles. The temperatures in the soil layer are obtained by solving the heat conduction equation. Appropriate boundary conditions are the heat energy balance at the soil surface and specification of the soil temperature at a certain depth.

The lateral boundary values are obtained by integrating the corresponding governing equations except that variations in the horizontal directions are all neglected.

An initial wind profile at the southwestern corner of the computational domain is first constructed by assuming a logarithmic variation (initially u_* = 0.2 m/s and z_o = 0.1 m) from the ground up to the level where the wind speed reaches an ambient value (2 m/s). Initial wind profiles at other grid locations are obtained by scaling the southwestern corner winds to satisfy mass continuity. Wind directions in the upper layers in summer over Japan are generally westerly. Thus, initial wind directions are assumed to be westerly everywhere.

Measurements by tethersondes indicate that the vertical gradients of potential temperature above the surface inversion layer are approximately 3.1 K/1000 m. Thus, the vertical profile of potential temperature is assumed to increase linearly with height: $\theta = 303 + 0.0031\ z$. Initial potential temperatures are assumed to be uniform in the horizontal directions. Initial values for water vapor are constructed by using the initial potential temperature profiles, pressure at the sea surface (1002 mb), and relative humidity, 50% (80% over the water) in the layers up to 2.4 km above the surface and 10% above that level. The turbulence kinetic energy and length scale are initialized by using the initial wind and temperature profiles, and the relationships obtained from the level 2 model. These expressions are already given by Yamada (1975) and are not repeated here.

The governing equations are integrated by using the Alternating Direction Implicit method (Richtmyer and Morton, 1967) and a time increment is chosen to satisfy the Courant-Friedrich-Lewy criteria. In order to increase the accuracy of finite-difference approximations, mean and turbulence variables are defined at grids which are staggered both in horizontal and vertical directions. Mean winds, temperature, and water vapor vary greatly with height near the surface. In order to resolve these variations, nonuniform grid spacings are used in the vertical direction. A grid of 39 x 41 x 16 (vertical) points is used to cover a computational volume of 380 x 400 x 7.3 km^3.

3. RESULTS

Integration is initiated at 5 a.m. and continued until 4 a.m. the following morning. Initially, wind directions are assumed westerly everywhere. The air temperature close to a sloped surface facing south or east becomes higher, due to the shortwave radiation heating from the sun, than the air temperature at the same height but away from the surface. This temperature difference results in a horizontal pressure gradient which moves air up the slope, i.e., valley winds. The valley winds are combined with sea-breeze circulations, resulting in two large mesoscale circulations: one from the Pacific Ocean and the other from the Japan Sea (Fig. 1). These circulations converge over the mountain ranges and form a clear front by 3 p.m. (Fig. 1). The modeled horizontal wind vectors and the convergence line are in good agreement with the measurements (Fig. 2 of Kurita and Ueda, 1986) obtained by the Automated Meteorological Data Acquition System (AMeDAS): a comprehensive surface meteorological network which covers Japan with instruments spaced on the average every 20 km. Vertical profiles of the modeled σ_w and potential temperature at station S1 (Fig. 1) are shown in Fig. 2. The modeled mixed layer depth is approximately 1000 m. This low mixed layer height limits vertical mixing of pollutants: a favorable condition for the long-range transport of pollutants.

In order to evaluate the relative importance of the sea-breeze circulations and the valley winds for long-range transport, two additional numerical simulations are performed: ocean is replaced by land in Case 2 and ground elevation is removed in Case 3. Figure 3 for Case 2 shows close resemblance to Fig. 1 (Case 1 where both topography and ocean are included), indicating topography is essential for generating circulations responsible for the long-range transport of pollutants from the coast to the mountainous region. On the other hand, Figure 4 for Case 3 with ground elevation removed shows little penetration of the sea-breeze, particularly in the Pacific Ocean coast region.

ACKNOWLEDGEMENTS

This work was supported by the U. S. Department of Energy. Authors are grateful to Dr. M. Williams for reviewing and Ms. K. Coen for typing the manuscript.

REFERENCES

Dyer, A. J. and B. B. Hicks, 1970: "Flux-Gradient Relationships in the Constant Flux Layer," Quart. J. Roy. Meteor. Soc. 96, 715-721.

Kurita H. Sasaki K., Muroga H., Ueda H. and Wakamatsu S. 1985: "Long-Range Transport of Air Pollution Under Light Gradient Wind Conditions. J. Clim. Appl. Met. 24, 425-434.

Kurita, H. and Ueda, H., 1986: "Meteorological Conditions for Long-Range Transport Under Light Gradient Winds. Atmos. Environ., 20, 687-694.

Richtmyer, R. D. and K. W. Morton, 1967: Difference Methods for Initial-Value Problems, Second Ed., Interscience Publishers, J. Wiley and Sons, New York, 405 pp.

Yamada, T., 1975: "The Critical Richardson Number and the Ratio of the Eddy Transport Coeffients Obtained from a Turbulence Closure Model," J. Atmos. Sci. 32, 926-933.

______________, 1985: "Numerical Simulations of the Night 2 Data of the 1980 ASCOT Experiments in the California Geysers Area," Archives for Meteorology, Geophysics, and Bioclimatology, Ser. A34, 223-247

______________, 1981: "A Numerical Simulation of Nocturnal Drainage Flow," J. Meteor. Soc. Japan, 59, 108-122.

Figure Captions

Fig. 1. The modeled horizontal wind vectors and a convergence line at 10 m above the ground at 3 p.m. Ground elevation is contoured at every 400 m with solid lines. The dashed lines indicate intermediate levels.

Fig. 2. Vertical profiles of the modeled σ_w and potential temperature at station S1 in Fig. 1.

Fig. 3. Same as for Fig. 1 except the ocean is replaced by land.

Fig. 4. Same as for Fig. 1 except the ground elevation is removed.

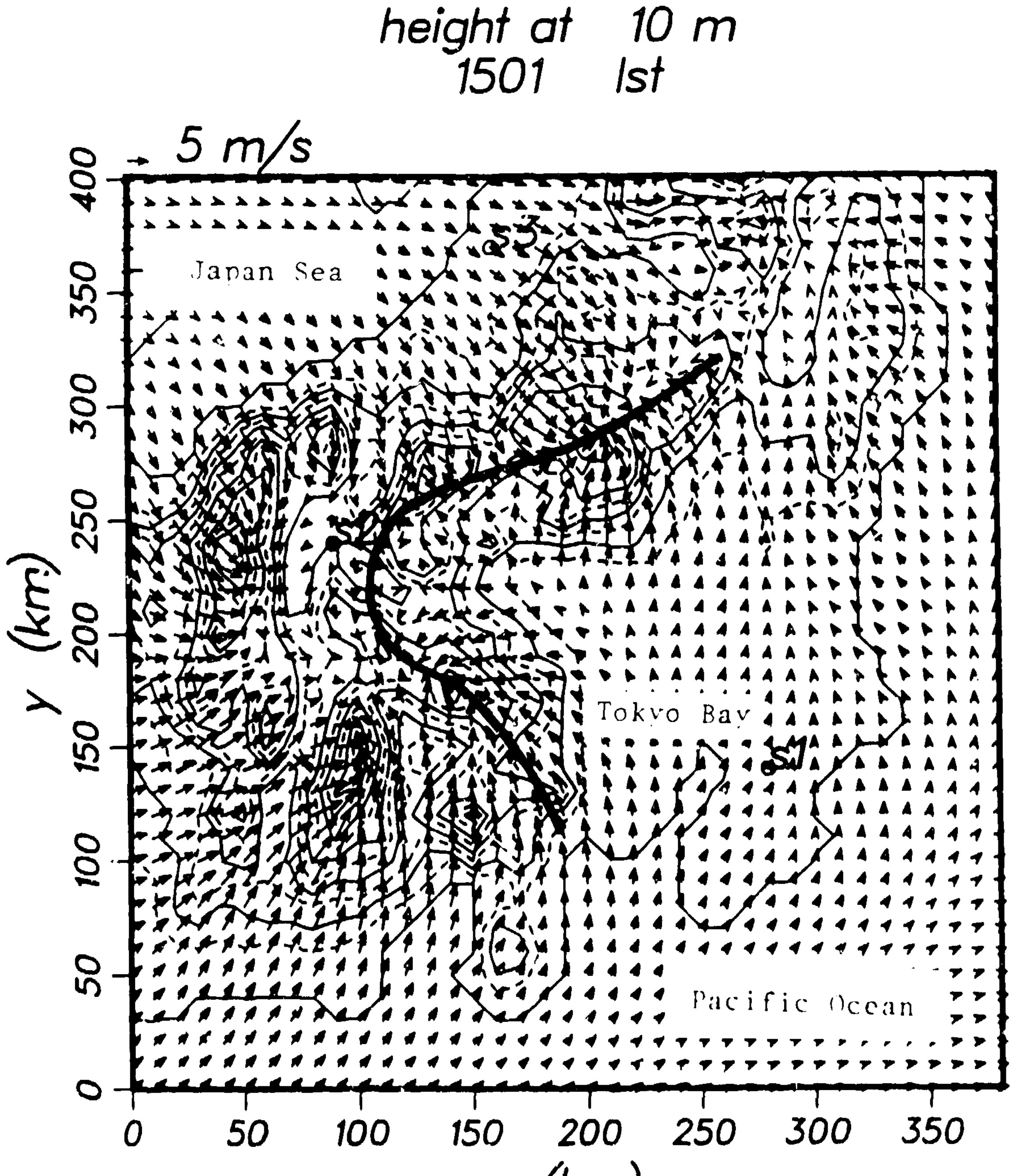

height at 10 m
1501 lst
5 m/s
Japan Sea
S3
Tokyo Bay
S1
Pacific Ocean
y (km)
x (km)
0
50
100
150
200
250
300
350
400

Fig. 1

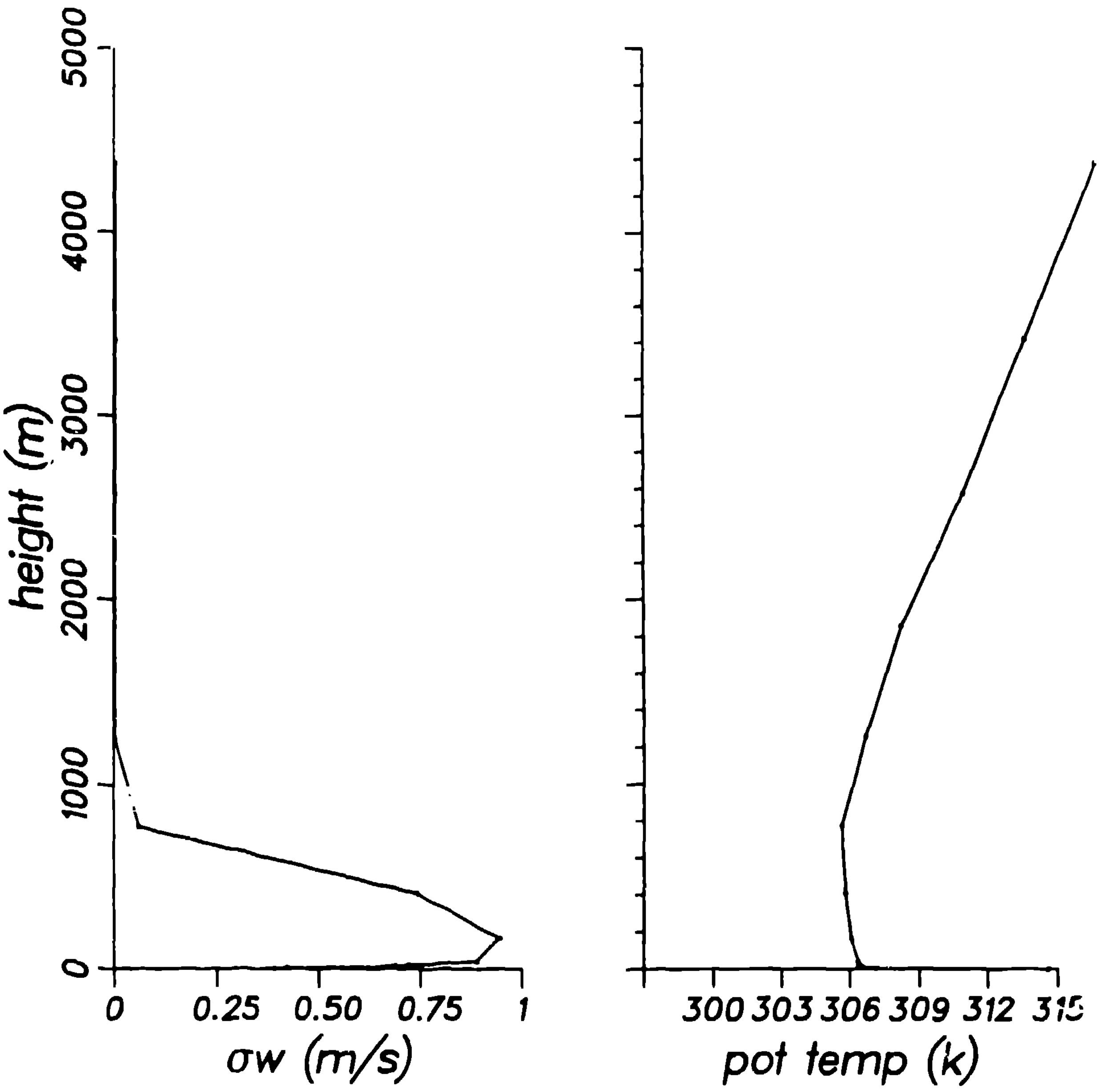
height (m)
0
1000
2000
3000
4000
5000
0
0.25
0.50
0.75
1
σw (m/s)
300 303 306 309 312 315
pot temp (k)

Fig. 2

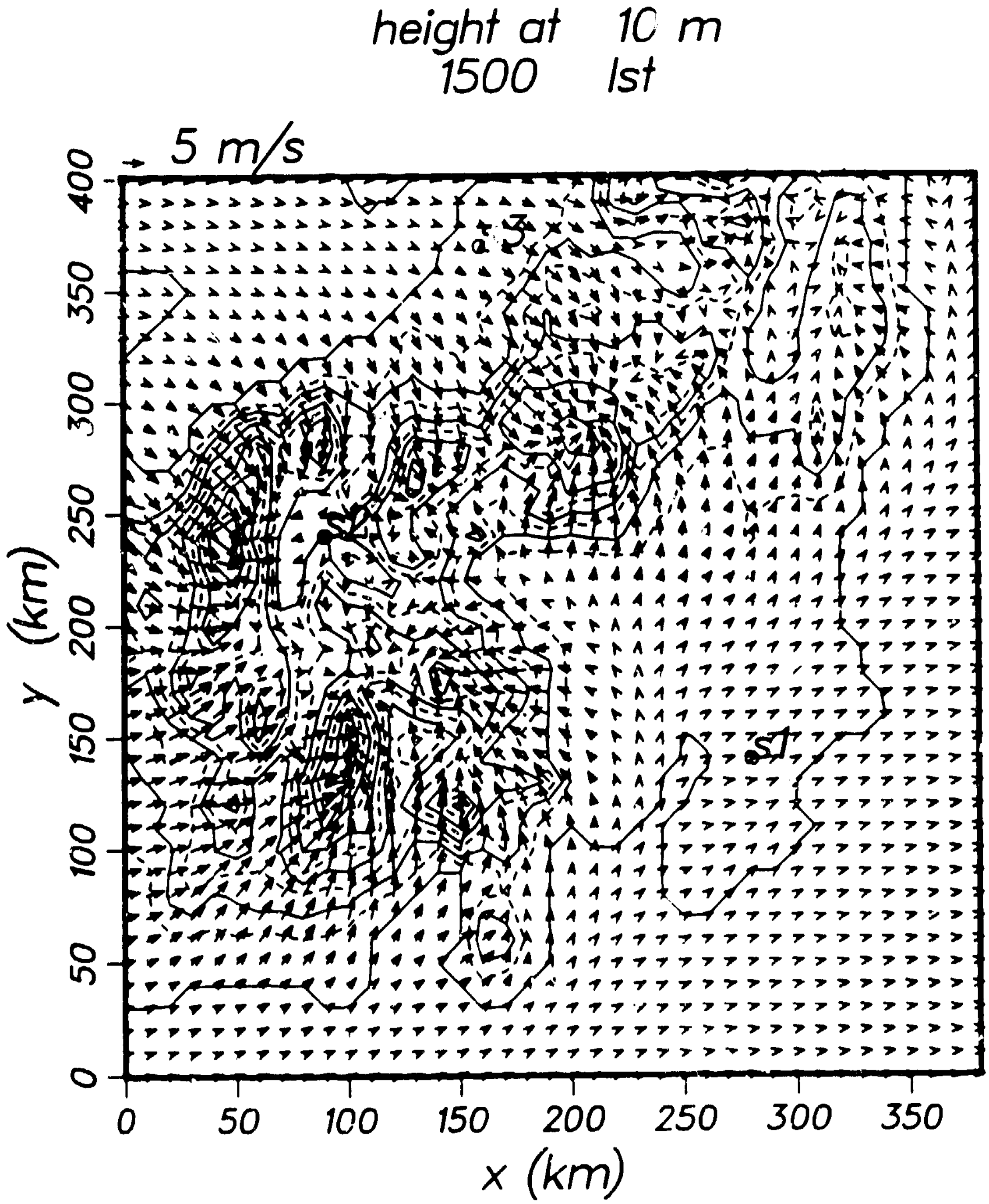
height at 10 m
1500 lst
5 m/s
y (km)
x (km)
0
50
100
150
200
250
300
350
400
s1
s2
s3

Fig. 5

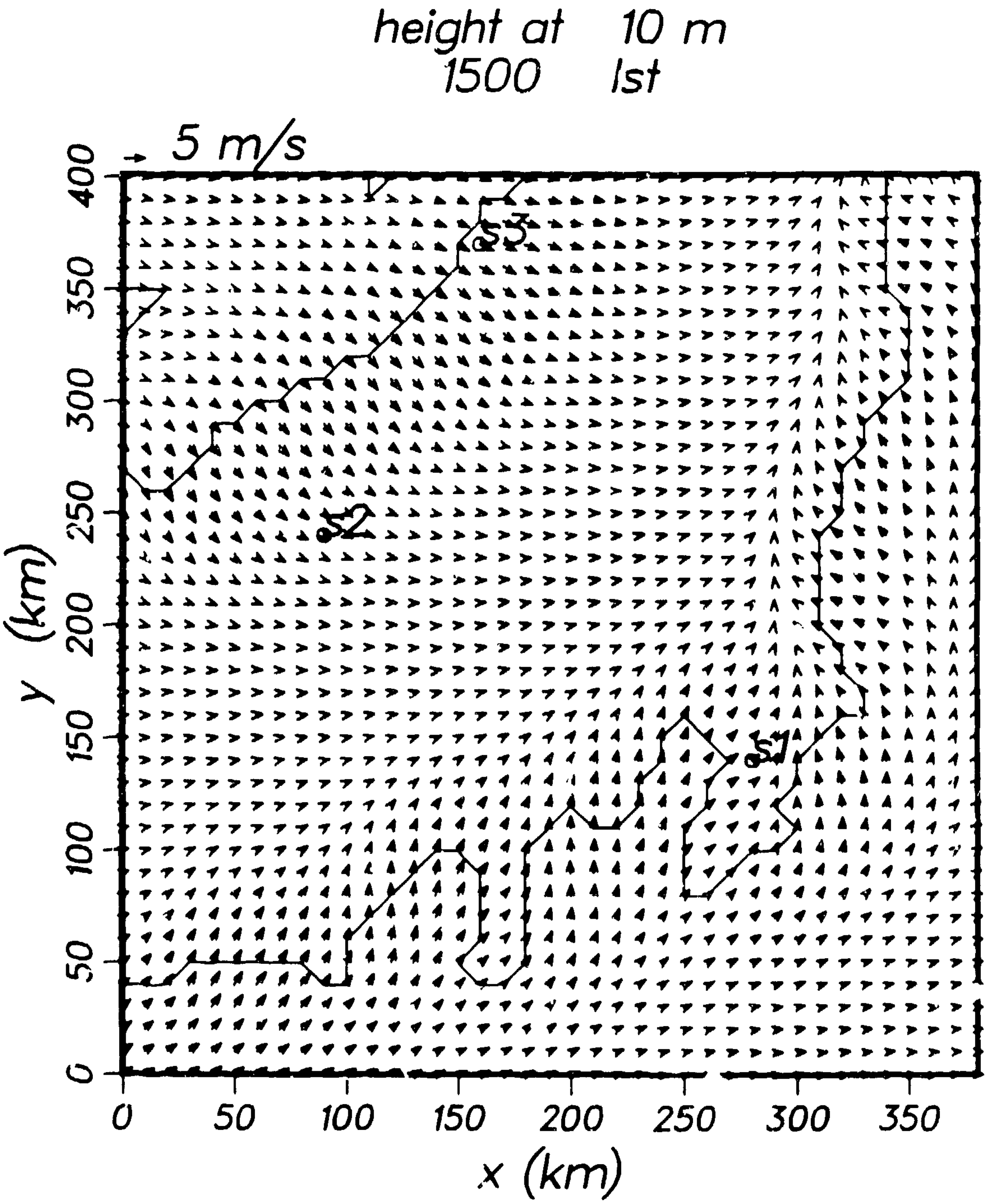
height at 10 m
1500 lst
5 m/s
S1
S2
S3
y (km)
x (km)
0
50
100
150
200
250
300
350
400

Fig. 4